Hydrogen-Transfer Reactions Examined in the Context of a Sputtered Ion Mechanism for Low-Energy Polyatomic Ion−Hydrocarbon Surface Collisions

Lynn M. Phelan,[†] **Mark J. Hayward,**[†,‡] **Julie C. Flynn,**[†] **and Steven L. Bernasek*,**[†]

Department of Chemistry, Princeton University, Princeton, New Jersey 08544, and Process and Analytical Research, American Cyanamid Company, Princeton, New Jersey

An associative ion/surface reaction channel has been observed in which hydrogen is attached to incident ions when low-energy polyatomic ions collide with hydrocarbon-covered surfaces. Since sputtered protons also are observed as a result of these collisions, the thermodynamics of hydrogen transfer have been examined for a series of polyatomic organic compounds and their ^{2}H-labeled analogues in the context of a sputtered ion mechanism. In this mechanism incident ions are neutralized via charge exchange with the adsorbate, releasing sputtered ions (protons), which then react with the neutralized incident ion to form the associative reaction product. If H addition proceeds via a sputtered ion mechanism, then the overall thermodynamics of this reaction should be related to the sum of the ionization potential (IP) and the proton affinity (PA) of the incident molecule. This hypothesis has been tested using the following series of compounds: phenol, toluene, benzene, cyclohexane, tetrahydrofuran, acetone, pyrazine, pyridine, and acetonitrile. It has been found that as the overall exothermicity for hydrogen addition increases (i.e., larger sum of IP and PA), the relative abundance of protonated molecular ions and sputtered proton-containing fragments increases. The threshold nature of the extent of hydrogen-transfer reaction as a function of IP + PA is suggestive of the reaction pathway involved in the sputtering of protons from hydrocarbon surfaces during SID MS/MS.

Introduction

Investigation of the interaction of gas-phase ions with surfaces is an area of increasing interest for both practical and fundamental reasons. Ion/surface collisions are used routinely for surface composition analysis using secondary ion mass spectrometry (SIMS).[1−4] There are also many important applications of ion/surface collisions in the microelectronics industry, including the use of focused ion beams (FIB) to remove or deposit material with great resolution (below 50 nm)[5] or for reactive etching of surfaces such as diamond,[6] which otherwise is difficult to do in a controllable manner. There are many other industrial applications including ion implantation of wear-resistant coatings such as titanium nitride,[7] which help to reduce friction, decreasing the need for environmentally harmful lubricants. Environmental and health concerns have also encouraged other advances using ion/surface collision implantation. Plasma source ion implantation (PSII) is used to harden and to increase the wear resistance of electrodeposited chromium,[8] reducing the release of carcinogenic Cr^{6+} into the environment.

In addition to compositional analysis and modification of the surface, ion/surface collisions can be used to probe the structure of the incident polyatomic ion. Studies of low-energy (10−100 eV) polyatomic ion/surface collisions are being carried out in order to develop a relatively new analytical technique, surface induced dissociation (SID) tandem mass spectrometry (MS/MS), which is used for probing structures of incident gas-phase ions. Applications of low-energy ion/surface collisions range from structural analysis of large ions (i.e., peptides), which are

difficult to fragment, to surface analysis through chemically specific ion/surface reactions. Fragmentation of peptides by SID is an area of considerable interest,[9−15] and SID has been important to understanding the energetics and fragmentation mechanisms of protonated peptides.[16] Work is emerging that describes surface composition analysis using specific ion/surface reactions as well.[17] However, even with these successes, the widespread use of SID MS/MS has not yet been realized, because little is known about the fundamentals of polyatomic ion/surface collisions at low collision energies, where the structure of ions are probed. Much of what is currently known has been described in reviews of the subject.[17−19]

Most SID experiments have been conducted by colliding low-energy (10−100 eV) polyatomic organic ions in high vacuum with either a hydrocarbon-covered (originating from pump oil) stainless steel surface[20,21] or a functionalized alkanethiol self-assembled monolayer surface (SAM).[22−24] Also, some recent work has been carried out in ultrahigh vacuum with well-characterized surface/adsorbate systems.[25−27] A variety of different reaction processes are possible when low-energy polyatomic ions collide with organic-covered surfaces.[18] Among the more interesting reaction processes are ones in which associative ion/surface products are formed. The most common associative reaction product and the subject of this paper is hydrogen addition to the incident molecular ion. A few different mechanistic views of associative ion/surface reaction product formation have been suggested. Originally, these associative ion/surface reactions were proposed to proceed via the combination of radical intermediates (presumably sputtered as the result of the collision of incident ions with the hydrocarbon overlayer) and the incident ion.[18,19] However, since more recent findings have established that these reactions involve charge exchange

* To whom correspondence should be addressed.
† Princeton University.
‡ American Cyanamid Co.

with the surface as a first step,[17] sputtered radicals may play far less of a role than originally thought.

Later, a concerted mechanism was proposed based on ab initio calculations and examination of the various associative reactions that occur when benzene and perdeuterated benzene collide with hydrocarbon SAM surfaces and fluorinated SAM surfaces.[24] However, some of the most recent work has provided considerable experimental evidence that a number of ion/surface associative reactions proceed via a sputtered ion mechanism.[29,30] In a sputtered ion mechanism, incident ions neutralize via charge exchange with surface species and produce sputtered ions. Upon collision the neutralized incident ions then react with the sputtered ions to form associative ion/surface reaction products as shown in the following reaction:

$$M^{\bullet+} + SA \rightarrow M + S + A^+ \rightarrow MA^+ + S \qquad (i)$$

where $M^{\bullet+}$ is the incident molecular ion, S is the substrate, and A is an attached surface species. Consistent observation of both the sputtered ion intermediates and the associative ion/surface products in the SID mass spectra makes a strong case for the sputtered ion mechanism.

In this paper, the associative ion/surface reaction that forms $[M+H]^+$ product ions from incident $M^{\bullet+}$ ions is studied in the context of the sputtered ion mechanism with emphasis being placed on the thermodynamics of this process. The qualitative thermodynamics of hydrogen addition have been examined previously in the context of a sputtered radical mechanism.[18,19] The work presented here quantitatively extends that approach by (1) considering the reaction to involve charge exchange as the first step as is now established,[17] (2) separating the mechanism into the energy components that hold constant and those that vary as the incident ion is varied, (3) using the trends in variable energy components to experimentally determine the threshold energy for the constant energy part of the reaction (proton sputtering), and (4) proposing a mechanism for proton sputtering based on this experimentally determined threshold energy. The results of this work are a clear demonstration that the extent of ion/surface hydrogen addition depends on the IP + PA of the incident ion, strong experimental support of the sputtered ion mechanism, and the detailed proposal of the entire reaction sequence involved in the ion/surface hydrogen addition reactions.
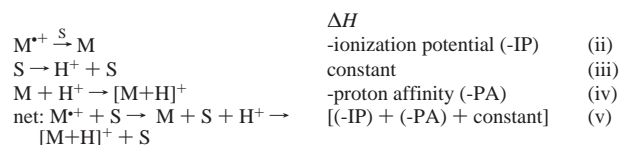
Experimental Section

The custom-built tandem quadrupole mass spectrometer used in these SID experiments has been described in detail previously.[29] The instrument is constructed from two Dycor M200M quadrupole mass spectrometers mounted in a custom 8 in. Conflat flange. One quadrupole serves as a differentially pumped mass-selective ion source. The other quadrupole serves as a scattered ion detector. A stainless steel surface (polished with 600 grit emery paper) is mounted with a specular collision angle of 108°. The instrument is operated with a standard electron impact (EI) ion source, electron multiplier detector, and Dycor data system. The spectrometer is mounted on a high-vacuum system with a base pressure of approximately 8×10^{-8} Torr, resulting in a scattering surface covered with adventitious hydrocarbons (originating from the pump oil). A unique feature of this tandem quadrupole instrument is its compact design. It has been designed to be readily mounted on a UHV surface analysis chamber, enabling studies in which the nature of the surface can be carefully controlled and characterized prior to and following the ion/surface collision.

SID studies of phenol, toluene, benzene, cyclohexane, tetrahydrofuran, acetone, acetonitrile, pyridine, pyrazine, and their perdeuterated analogues were carried out. Benzene, pyridine, toluene, tetrahydrofuran, phenol, cyclohexane, and acetone were obtained from EM Science, acetonitrile from Baker, and pyrazine, pyrazine-d_4, acetone-d_6, phenol-d_6, and cyclohexane-d_{12} from Aldrich. The remaining perdeuterated samples were obtained from Cambridge Isotope. Samples were introduced through a custom batch inlet after being subjected to several freeze−pump−thaw cycles. All samples had a high enough vapor pressure to be used at room temperature and were introduced into the differentially pumped ion source using a Varian variable-leak valve. Ion currents at the surface were approximately 1 nA.

SID mass spectra for each compound were recorded using two different lens-tuning procedures. In the first set of experiments the instrument was tuned for each compound independently, so as to maximize both the surface current and the product ion spectra. In a second set of experiments intended to better allow direct comparison of spectra, the instrument was tuned initially using benzene, again, maximizing the surface current and product ion spectra obtained. These tuning parameters were then kept constant and used to record the SID mass spectra for the rest of the compounds. Close examination revealed that simply using the same tuning conditions for all compounds (as opposed to tuning for each sample) yielded similar spectra. By using the same potentials, the time required to acquire the spectra was reduced substantially, allowing better comparison of spectra and reducing errors that might be attributed to changing conditions in the vacuum system. In both sets of SID experiments 10 spectra for each compound were averaged using peak heights for intensity measurements. Both experimental conditions yielded similar results. All measurements were repeated several times on different days in order to ensure their repeatability.

Results

Previous work has described the observation of sputtered protons (m/z 1) when polyatomic ions collide with a hydrocarbon-covered stainless steel surface.[29] In addition, it is well-known that neutralization of the incident ion beam is significant in these types of collisions.[18,19] When combined, these two key observations suggest that the formation of protonated molecular ions may result from reaction of sputtered protons with neutralized incident molecular ions (i.e., via a sputtered ion mechanism). The thermodynamics of the sputtered ion mechanism for hydrogen transfer might be viewed as shown in the following simple model:

	ΔH	
$M^{\bullet+} \xrightarrow{S} M$	-ionization potential (-IP)	(ii)
$S \rightarrow H^+ + S$	constant	(iii)
$M + H^+ \rightarrow [M+H]^+$	-proton affinity (-PA)	(iv)
net: $M^{\bullet+} + S \rightarrow M + S + H^+ \rightarrow$ $[M+H]^+ + S$	$[(-IP) + (-PA) + \text{constant}]$	(v)

The first step is the neutralization of the incident ion ($M^{\bullet+}$) by electron transfer. It is generally accepted that these reactions occur by first charge exchanging with the surface.[17] This is followed by sputtering of a proton (H^+) from the surface (S). In this model the surface energetics are intentionally simplified and assumed constant so that the ion energetics may be examined in sufficient detail to later infer information about the surface energetics. Finally, the reaction of neutralized incident ions with the sputtered protons yields the protonated

Hydrogen-Transfer Reactions

J. Phys. Chem. B, Vol. 102, No. 29, 1998 **5669**

TABLE 1: Thermodynamic Values for the Series of Compounds Studied[a]

	PA (kJ/mol)	IP (kJ/mol)	-PA − IP (kJ/mol)
phenol	821	816	−1637
toluene	794	850	−1644
benzene	759	890	−1649
cyclohexane	707	950	−1657
tetrahydrofuran	832	907	−1739
acetone	823	935	−1758
pyrazine	874	895	−1769
pyridine	924	891	−1815
acetonitrile	834	1174	−2008

[a] All proton affinity values and ionization potentials were obtained from ref 31 with PA values defined at 298 K and IP values adiabatic and defined at 0 K.

product ([M+H]$^+$). There are several key assumptions in this proposed model. First, it is assumed that the surface is covered with hydrocarbon (adventitious pump oil) and the overall nature of the surface is constant over the course of the experiments. The next assumption is that the heat of reaction for forming sputtered protons is constant for the range of molecular ions examined at constant collision energy, which, as will be shown later in this paper, is necessary in order to gain information from the experimental trends on the nature of proton production. The final assumption in this thermodynamic analysis is that the proton-transfer reaction occurs prior to any unimolecular dissociation that may occur. Considering the reaction sequence in this way suggests that the relative extent of protonation should be related to the sum of the ionization potential and the proton affinity of the neutralized molecular ion. This is important because it separates the known incident ion energetics from the unknown surface energetics, and if the assumptions about the mechanistic model are correct, then the extent of reaction trends as a function of the known ion energetics given in Table 1[31] (IP + PA) also should yield information about the unknown surface energetics.

To experimentally test the mechanistic model, nine compounds (Table 1) were chosen for SID examination with two criteria in mind. The first is that the corresponding thermodynamics of ionization and protonation span a reasonably broad range of energies.[31] The second is that the perdeuterated compounds be readily available. By examining both the unlabeled and perdeuterated versions of the compounds, it is possible to separtate the various interaction processes (i.e., elastic scattering, chemical sputtering, dissociation, and associative reactions) that are seen in a typical SID mass spectrum. An example of the type of spectra obtained is shown in Figure 1 for acetone-d_6. The use of ^{2}H-labeled compounds facilitates peak assignments, because all fragment ions that originate directly from the molecular ion appear at even mass-to-charge ratios (for non-nitrogen containing compounds). Thus, odd mass peaks in the spectra of a ^{2}H-labeled compound must contain a portion of the surface. These odd mass ions must be either ion surface H addition products or hydrocarbons sputtered from the surface. Sputtered ion peaks are readily identified since their masses and intensities remain constant for both the spectra for unlabeled and ^{2}H-labeled compounds. Peak assignments and relative abundances are given in the Supporting Information for each of the compounds examined.

Assigning peaks in this way has allowed the relative abundance of the various processes (i.e., elastic scattering, ion/ surface associative reactions, sputtering, and fragmentation of the molecular ion and protonated molecular ion) to be determined. The relative abundances for each process can then be examined as a function of the known energetics for the
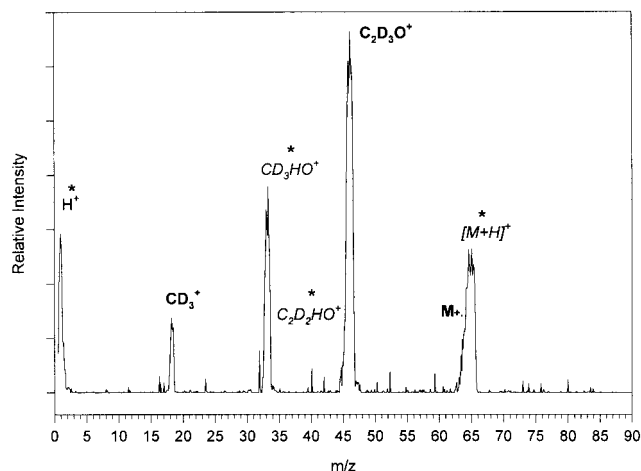
d-6 acetone 30eV

Figure 1. 30 eV SID mass spectrum of acetone-d_6. Peaks denoted with an asterisk contain surface hydrogen.

mechanistic model in order to test its validity. As part of these tests, it might seem useful to monitor the sputtered proton peak intensity compared to the extent of hydrogen transfer. However, this is experimentally difficult because tuning conditions of the instrument are vastly different for the very low mass ions compared to the mass region m/z 15 or greater; that is, the tuning conditions used for obtaining the incident ion dissociation products are far from the optimum tuning for sputtered protons. In addition, the sputtered protons may undergo other competing reactions that cannot be monitored, such as the formation of neutral products. This makes any direct quantitative comparisons difficult to interpret. In this work, we have found it useful to examine two sets of processes in order to better understand hydrogen addition during SID. One process considered is intact scattering (i.e., comparison of M$^{•+}$ and [M+H]$^+$ abundances) and the other is fragmentation (i.e., comparison of surface proton- and non-proton-containing fragment ion abundances for perdeuterated incident ions). Correlating data from these processes with thermodynamic data (IP + PA values) is suggestive of the mechanism involved in hydrogen addition.

The abundance of the [M+H]$^+$ ion, an ion/surface associative reaction product, can be directly compared to the relative abundance of the molecular ion. The ratio of protonated molecular ion ([M+H]$^+$) signal to molecular ion (M$^{•+}$) signal gives an experimentally determined extent of protonation. In Figure 2 the extent of protonation is correlated with the thermodynamics of protonation based on the sputtered ion mechanism by plotting M$^{•+}$/ [M+H]$^+$ versus (IP + PA). As seen in Figure 2, the least favorable overall enthalpy of protonation in this series of compounds (phenol) corresponds to the least amount of protonation observed (i.e., the largest M$^{•+}$/[M+H]$^+$ ratio). The trend in the data is clearly in agreement with the thermodynamic description of the sputtered ion mechanism for the formation of the [M+H]$^+$ ion. It is important to note that the trend is observed only as a function of the sum of the ionization potential *and* the proton affinity of the incident ion. There is no observed correlation with either thermodynamic parameter considered separately.

Fragmentation products observed in an SID spectrum may originate from different sources. One source is the direct fragmentation of the incident molecular ion and another is the subsequent fragmentation of the ion/surface reaction product, [M+H]$^+$ ion (assuming that proton transfer occurs prior to
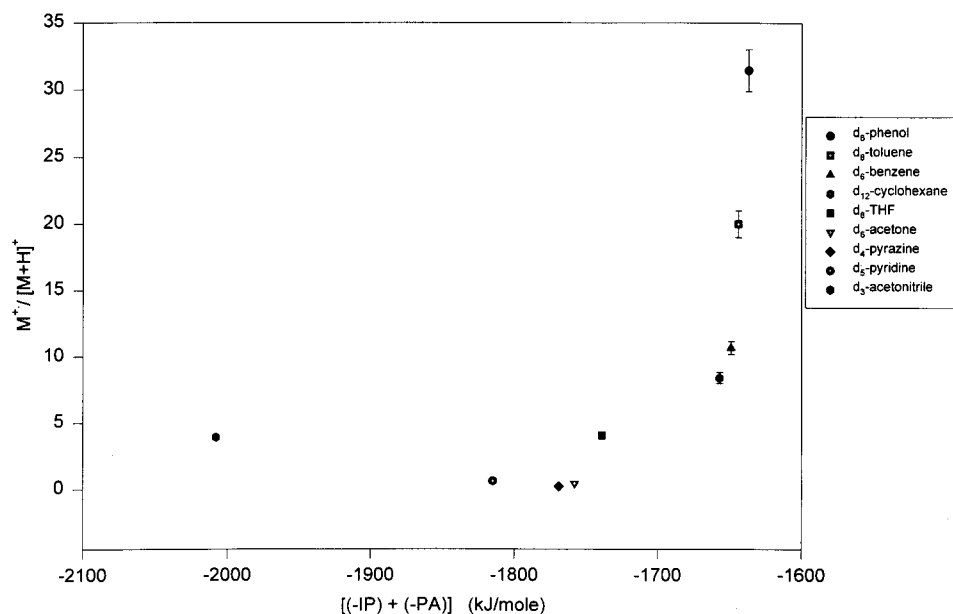
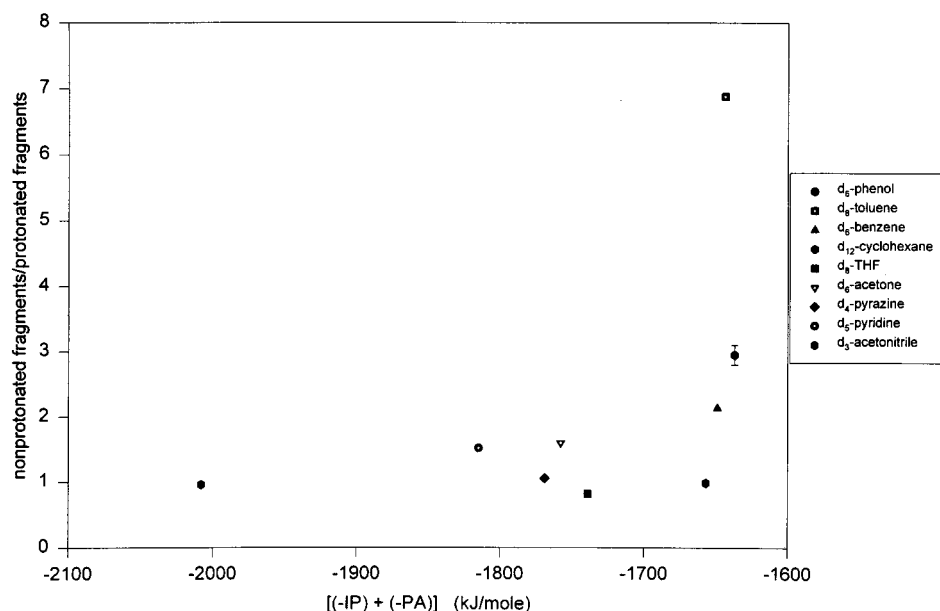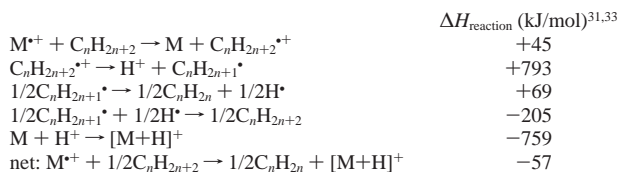**Figure 2.** $M^{\bullet+}/[M+H]^+$ vs $[(-IP) + (-PA)]$ plot.

Figure 3. Nonprotonated fragments/protonated fragments vs $[(-IP) + (-PA)]$ plot.

dissociation). In each of the spectra for the compounds examined, there is evidence for both of these processes. In Figure 3, the ratio of the non-proton-containing fragment ion signal to the proton-containing fragment ion signal is plotted as a function of the sum of IP and PA (known ion energetics based on the sputtered ion mechanism). Note that the trend exhibited by the ratios of nonprotonated fragments to protonated fragments in Figure 3 is similar to that which was observed for the $M^{\bullet+}/[M+H]^+$ ratio, again supporting the sputtered ion mechanism. In general for this series of compounds, the more exothermic the protonation reaction of the molecular ion, the greater the relative abundance of the observed protonated fragments. These results have several important implications for the relative importance of key parameters of the proposed sputtered ion mechanism. The first is that the assumption made in the model, that protonated fragments come primarily from the $[M+H]^+$ ion (and not from protonated neutrals), appears to be valid. Another conclusion, based on the observed similar trends for the parent ion ratios and the fragment ion ratios, is

that the sum of IP and PA is the primary energetic driving force in this mechanism. Other possible factors such as fragmentation efficiency differences between the $M^{\bullet+}$ and $[M+H]^+$ (and fragmentation efficiency differences between compounds), uncertainty in experimental and thermodynamic values, and mass-dependent discrimination of the quadrupole mass filter appear to have minimal effect on the overall observed trend.

Both Figures 2 and 3 exhibit a consistent threshold behavior in the plots of ion ratios versus the sum of IP and PA. The relatively smooth trends and the consistent threshold suggest that the model given in reactions ii through v is valid in assuming a constant energy reaction process for the sputtering of protons in the formation of hydrogen addition product ions. As the hydrogen addition becomes less thermodynamically favorable, the measured ion ratios $M^{\bullet+}/[M+H]^+$ and nonprotonated to protonated fragments ratio increase dramatically at a value of the sum of IP and PA of approximately 1600 kJ/mol. Since the model chosen (reactions ii through v) separates the ion energetics from the surface energetics, this value should

provide a reasonable estimate of the energy required for the proton sputtering step in hydrogen-transfer reactions, which is assumed constant in the thermodynamic analysis of the sputtered ion mechanism presented here. By assuming that 1600 kJ/mol is the energy required to sputter protons from hydrocarbon surfaces, one can then use this information to suggest the reaction pathway involved in proton sputtering. After considering a variety of pathways, a reaction route has been found that closely matches the experimentally indicated 1600 kJ/mol of energy required for proton sputtering. The reaction route is as follows:

	$\Delta H_{reaction}$ (kJ/mol)[31,33]
$M^{\bullet+} + C_nH_{2n+2} \rightarrow M + C_nH_{2n+2}^{\bullet+}$	+45
$C_nH_{2n+2}^{\bullet+} \rightarrow H^+ + C_nH_{2n+1}^{\bullet}$	+793
$1/2C_nH_{2n+1}^{\bullet} \rightarrow 1/2C_nH_{2n} + 1/2H^{\bullet}$	+69
$1/2C_nH_{2n+1}^{\bullet} + 1/2H^{\bullet} \rightarrow 1/2C_nH_{2n+2}$	−205
$M + H^+ \rightarrow [M+H]^+$	−759
net: $M^{\bullet+} + 1/2C_nH_{2n+2} \rightarrow 1/2C_nH_{2n} + [M+H]^+$	−57

$M^{\bullet+}$ is the incident ion and C_nH_{2n+2} is a hydrocarbon at the surface. The $\Delta H_{reaction}$ calculated above is specifically for benzene molecular cations incident on C_8H_{18} and the *n* isomer for C_8H_{16}, 2-octene, which suggests that H addition is slightly exothermic for benzene molecular ions. This reaction is relatively independent of the surface hydrocarbon chain length,[30] making the thermodynamic values for C_8H_{18} suitable for this analysis. Note that this reaction pathway involves mobile hydrogen atoms which react to stabilize alkyl radicals and is consistent with a previous suggestion[30] that mobile hydrogen atoms are involved in stabilizing hydrocarbon surface radicals that result from the sputtering process. Using the gas-phase ΔH values above, the model thermodynamic cycle gives a value of 1592 kJ/mol for the enthalpy of the proton sputtering step in the sputtered ion mechanism, which is in excellent agreement with the 1600 kJ/mol experimentally observed threshold value.

Conclusion

To investigate hydrogen addition reactions in the context of a sputtered ion mechanism, SID spectra have been recorded for a series of polyatomic organic ions (and their ^{2}H-labeled analogues) with a range of hydrogen addition energies (i.e., the sum of IP and PA). Based on $M^{\bullet+}/[M+H]^+$ ratios, it has been observed that the more exothermic the hydrogen transfer reaction, the greater the relative extent of hydrogen addition to incident molecular cations. In addition, examination of the ratio of the sum of relative abundances of the protonated and nonprotonated fragment ions shows a clear trend where the extent of protonation is greater when the reaction is more exothermic. The agreement of this trend with the $M^{\bullet+}/[M+H]^+$ ratio suggests that most of the protonated fragments come from the $[M+H]^+$ ion and not protonated neutral fragments. Furthermore, these smooth trends and the threshold behavior at 1600 kJ/mol suggest that the same independent proton generating process is involved in the formation of all of the surface proton containing species for all of the compounds examined. The observed threshold for this reaction is indicative of the reaction route for proton sputtering and is consistent with the previous hypothesis[30] that mobile hydrogen atoms react to stabilize alkyl radicals produced as part of the sputtering process. Each of these three important results provides strong support for a sputtered ion mechanism (reaction i) for the formation of $[M+H]^+$ ions when low energy polyatomic molecular cations collide with a hydrocarbon-covered surface. While other possible reaction routes cannot be completely ruled out, when these results are combined with the observation of sputtered

protons in great abundance[29,30] and the well-known fact that a considerable portion of the incident ions are neutralized,[17−19] the sputtered ion mechanism for hydrogen addition seems a very likely candidate for the actual mechanism producing $[M+H]^+$ ions (from $M^{\bullet+}$) in SID.

This work provides another demonstration that gas-phase thermodynamic models along with the existing base of gas-phase reaction energies available from the literature are valid and useful tools for understanding the mechanisms and driving forces leading to ion surface reaction products.[30] In turn, this simplification of the understanding of associative ion surface reaction mechanisms should help lead to greater acceptance of low-energy ion−surface collisions for routine analytical purposes.

References and Notes

(1) Benninghoven, A. *Surf. Sci.* **1994**, *299-300*, 246.

(2) Newman, A. *Anal. Chem.* **1996**, *68*, 683.

(3) Leggett, G. J.; Davies, M. C.; Jackson, D. E. *J. Phys. Chem.* **1993**, *97*, 5348.

(4) Ray, M. A.; Baker, J. E.; Loxton, C. M.; Green, J. E. *J. Vac. Sci. Technol.* **1988**, *A6*, 44 .

(5) Stevie, F. A.; Shane, T. C.; Kahora, P. M.; Hull, R.; Bahnck, D.; Kannan, V. C.; David, E. *Surf. Interface Anal.* **1995**, *23*, 61.

(6) Sandhu, G. S.; Chu, W. K. *Appl. Phys. Lett.* **1989**, *55*, 437.

(7) Seidel, F.; Stock, H.-R.; Mayr, P. *Surf. Coat. Technol.* **1996**, *84*, 506.

(8) Walter, K. C.; Scheuer, J. T.; McIntyre, P. C.; Kodali, P.; Yu, N.; Nastasi, M. *Surf. Coat. Technol.* **1996**, *85*, 1.

(9) Cooks, R. G.; Amy, J. W.; Bier, M. E.; Schwartz, J. C.; Schey, K. L. *Adv. Mass Spectrom.* **1989**, *11*, 33.

(10) McCormack, A. L.; Somogyi, A.; Dongre, A. R.; Wysocki, V. H. *Anal. Chem.* **1993**, *65*, 2859.

(11) McCormack, A. L.; Jones, J. L.; Wysocki, V. H. *J. Am. Soc. Mass Spectrom.* **1992**, *3*, 859.

(12) Jones, J.; Dongre, A. R.; Somogyi, A.; Wysocki, V. H. *J. Am. Chem. Soc.* **1994**, *116*, 8368.

(13) Wright, A. D.; Despeyroux, D.; Jennings, K. R. *Org. Mass Spectrom.* **1992**, *27*, 525.

(14) Despeyroux, D.; Wright, A. D.; Jennings, K. R. *Int. J. Mass Spectrom. Ion Processes* **1993**, *126*, 95.

(15) Cole, R. B.; LeMeillour, S.; Tabet, J. C. *Anal. Chem.* **1992**, *62*, 365.

(16) Dongre, A. R.; Somogyi, A.; Wysocki, V. H. *J. Mass Spectrom.* **1996**, *31*, 339.

(17) Cooks, R. G.; Ast, T.; Pradeep, T.; Wysocki, V. H. *Acc. Chem. Res.* **1994**, *27*, 316.

(18) Cooks, R. G.; Ast, T.; Md. Mabud, A. *Int. J. Mass Spectrom. Ion Processes* **1990**, *100*, 209.

(19) Ast, T.; Md. Mabud, A.; Cooks, R. G. *Int. J. Mass Spectrom. Ion Processes* **1988**, *82*, 131.

(20) Bier, M. E.; Schwartz, J. C.; Schey, K. L.; Cooks, R. G. *Int. J. Mass Spectrom. Ion Processes* **1990**, *103*, 1.

(21) Md. Mabud, A.; Dekrey, M. J.; Cooks, R. G. *Int. J. Mass Spectrom. Ion Processes* **1985**, *67*, 286.

(22) Winger, B. E.; R. K. Julian Jr., Cooks, R. G. *J. Am. Chem. Soc.* **1991**, *113*, 8967.

(23) Morris, M. R.; Riederer, D. E., Jr.; Winger, B. E.; Cooks, R. G.; Ast, T.; Chidsey, C. *Int. J. Mass Spectrom. Ion Processes* **1992**, *122*, 181.

(24) Somogyi, A.; Kane, T. E.; Ding, J.; Wysocki, V. H. *J. Am. Chem. Soc.* **1993**, *115*, 5275.

(25) Wu, Q.; Hanley, L. *J. Phys. Chem.* **1993**, *97*, 8021.

(26) Wu, Q.; Hanley, L. *J. Phys. Chem.* **1993**, *97*, 2677.

(27) Burroughs, J. A.; Wainhaus, S. B.; Hanley, L. *J. Phys. Chem.* **1994**, *98*, 10913.

(28) Hayward, M. J.; Md. Mabud, A.; Cooks, R. G. *J. Am. Chem. Soc.* **1988**, *110*, 1343.

(29) Hayward, M. J.; Park, F. D. S.; Manzella, L. M.; Bernasek, S. L. *Int. J. Mass Spectrom. Ion Processes* **1995**, *148*, 25.

(30) Hayward, M. J.; Park, F. D. S.; Phelan, L. M.; Bernasek, S. L.; Somogyi, A.; Wysocki, V. H. *J. Am. Chem. Soc.* **1996**, *118*, 8375.

(31) *J. Phys. Chem. Ref. Data* **1988**, *V17*, Suppl. 1.

(32) Wysocki, V. H.; Jones, J. L.; Ding, J. M. *J. Am. Chem. Soc.* **1991**, *113*, 8969.

(33) Mautner, M.; Sieck, L. W.; Ausloos, P. *J. Am. Chem. Soc.* **1981**, *103*, 5342